

Growths of staggered InGaN quantum wells light-emitting diodes emitting at 520–525 nm employing graded growth-temperature profile

Hongping Zhao, Guangyu Liu, Xiao-Hang Li, G. S. Huang, Jonathan D. Poplawsky et al.

Citation: *Appl. Phys. Lett.* **95**, 061104 (2009); doi: 10.1063/1.3204446

View online: <http://dx.doi.org/10.1063/1.3204446>

View Table of Contents: <http://apl.aip.org/resource/1/APPLAB/v95/i6>

Published by the [American Institute of Physics](http://www.aip.org).

Related Articles

ZnO nanorods-graphene hybrid structures for enhanced current spreading and light extraction in GaN-based light emitting diodes

Appl. Phys. Lett. **100**, 061107 (2012)

Electrically driven nanopillar green light emitting diode

Appl. Phys. Lett. **100**, 061106 (2012)

Ultraviolet electroluminescence from colloidal ZnO quantum dots in an all-inorganic multilayer light-emitting device

Appl. Phys. Lett. **100**, 061104 (2012)

Organic light-emitting diodes for lighting: High color quality by controlling energy transfer processes in host-guest-systems

J. Appl. Phys. **111**, 033102 (2012)

Effect of the graded electron blocking layer on the emission properties of GaN-based green light-emitting diodes

Appl. Phys. Lett. **100**, 053504 (2012)

Additional information on *Appl. Phys. Lett.*

Journal Homepage: <http://apl.aip.org/>

Journal Information: http://apl.aip.org/about/about_the_journal

Top downloads: http://apl.aip.org/features/most_downloaded

Information for Authors: <http://apl.aip.org/authors>

ADVERTISEMENT



LakeShore Model 8404 developed with **TOYO Corporation**
NEW AC/DC Hall Effect System Measure mobilities down to 0.001 cm²/V s

Growths of staggered InGaN quantum wells light-emitting diodes emitting at 520–525 nm employing graded growth-temperature profile

Hongping Zhao,^{1,a)} Guangyu Liu,¹ Xiao-Hang Li,¹ G. S. Huang,¹ Jonathan D. Poplawsky,² S. Tafon Penn,² Volkmar Dierolf,² and Nelson Tansu^{1,b)}

¹Department of Electrical and Computer Engineering, Center for Optical Technologies, Lehigh University, Bethlehem, Pennsylvania 18015, USA

²Department of Physics, Center for Optical Technologies, Lehigh University, Bethlehem, Pennsylvania 18015, USA

(Received 27 May 2009; accepted 21 July 2009; published online 12 August 2009)

Three-layer staggered InGaN quantum wells (QWs) light-emitting diodes (LEDs) emitting at 520–525 nm were grown by metal-organic chemical vapor deposition by employing graded growth-temperature profile. The use of staggered InGaN QW, with improved electron-hole wave functions overlap design, leads to an enhancement of its radiative recombination rate. Both cathodoluminescence and electroluminescence measurements of three-layer staggered InGaN QW LED exhibited enhancements by 1.8–2.8 and 2.0–3.5 times, respectively, over those of conventional InGaN QW LED. © 2009 American Institute of Physics. [DOI: 10.1063/1.3204446]

High-efficiency InGaN based quantum wells (QWs) light emitting diodes (LEDs) play an important role in solid-state lighting.^{1–4} The existence of polarization fields in InGaN QW lead to charge separation in the QW, which significantly reduces the electron-hole wave function overlap ($\Gamma_{e,hh}$) and radiative recombination rate ($\sim |\Gamma_{e,hh}|^2$) of the InGaN QW. The commonly used approaches to extend the emission wavelength of conventional InGaN QW into the green spectral regime ($\lambda > 525$ nm) are as follows: (1) increase In-content in InGaN QW or (2) increase thickness of the InGaN QW. Both approaches lead to detrimental charge separation effect. Recently, several approaches have been proposed to address the charge separation issues in InGaN QW by employing nonpolar InGaN QW,⁵ InGaN QW with AlGaIn δ -layer,^{6,7} staggered InGaN QW,^{8,9} type-II InGaN-GaNAs QW,^{10,11} and strain-compensated InGaN-AlGaIn QW.^{12,13}

In this work, we present the growths and characteristics of three-layer staggered InGaN QW LEDs emitting in the 520–525 nm spectral regime employing graded growth-temperature profile, with the QW structure designed for improved overlap $\Gamma_{e,hh}$. Previously, the two-layer staggered InGaN QW^{8,9} was employed for 460 nm emitting LEDs, and the In-contents in QWs were engineered by changing the [TMIn]/[TEGa] molar flux ratios during the InGaN QW growth. For low In-content InGaN QWs applicable for blue-emitting LEDs, the In-content can be modified by changing the [TMIn]/[TEGa] molar flux ratio. However, for high In-content InGaN QWs applicable for green-emitting LEDs, the compositional engineering of the In-contents in the QW layers is most efficiently accomplished by grading the growth temperature.

In our current studies, the three-layer staggered InGaN QW LEDs were grown by metal-organic chemical vapor deposition (MOCVD) with graded growth-temperature profile [Fig. 1(a)] while keeping constant [TMIn]/[TEGa] molar ratio. The incorporation of indium into the InGaN layer is

very sensitive to the growth temperature. As shown in Fig. 1(a), the three-layer staggered $\text{In}_x\text{Ga}_{1-x}\text{N}/\text{In}_y\text{Ga}_{1-y}\text{N}/\text{In}_x\text{Ga}_{1-x}\text{N}$ QW structure is composed of three layers (layers 1, 2, and 3). The growth condition for the three-layer staggered InGaN QW is designed as follows: layer 1 is grown at T_1 (°C) for t_1 (s), layer 2 is grown at T_2 (°C) for t_2 (s), and layer 3 is grown at T_1 (°C) for t_1 (s). Between the layers 1 and 2, the temperature is ramped up from T_1 (°C) to T_2 (°C) by t_p (s). In contrast, between layers 2 and 3, the temperature

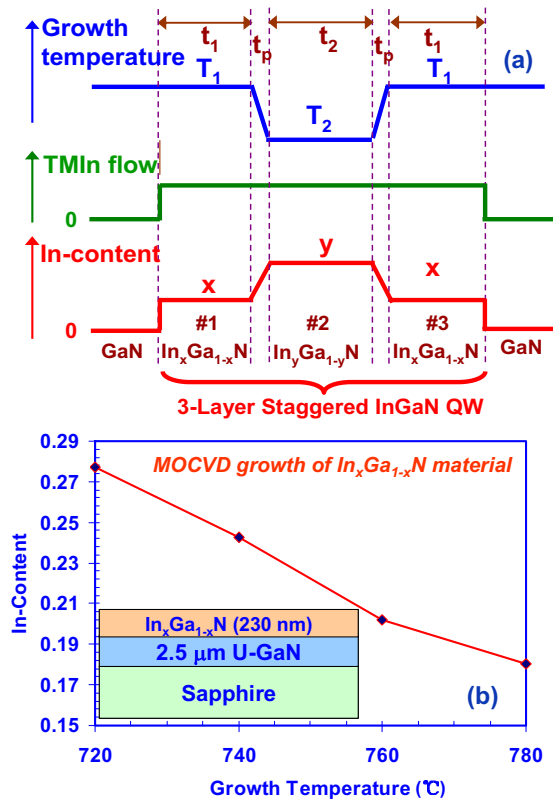


FIG. 1. (Color online) (a) Schematics of the growth temperature, TMIn-flow rate, and In-content for the growths of three-layer staggered InGaN QW with graded growth-temperature profiles and (b) the In-contents in MOCVD-grown $\text{In}_x\text{Ga}_{1-x}\text{N}$ layer as a function of growth temperature.

^{a)}Electronic mail: hoz207@lehigh.edu.

^{b)}Electronic mail: tansu@lehigh.edu.

is ramped down from T_2 ($^{\circ}\text{C}$) to T_1 ($^{\circ}\text{C}$) by t_p (s). The real growth temperature profile contains brief overshoot during the ramp-up and ramp-down layer growths. By utilizing the graded growth-temperature profile, the composition of In-content in the InGa N layer can be engineered to form three-layer staggered InGa N QW structure.

Numerical models based on self-consistent six-band $k \cdot p$ formalism for wurtzite semiconductor^{13–17} were employed to optimize the spontaneous emission characteristics of staggered InGa N QW. The simulation predicts that the use of three-layer staggered InGa N QW, instead of two-layer staggered InGa N QW, leads to further improvement in its overlap Γ_{e_hh} .¹⁴ For the optimized three-layer staggered InGa N QW ($\Gamma_{e_hh}=29.9\%$) emitting at 525 nm, the overlap Γ_{e_hh} is improved by 15% in comparison to that of the optimized two-layer staggered InGa N QW ($\Gamma_{e_hh}=26.3\%$). The conventional InGa N QW emitting at 525 nm has relatively low overlap ($\Gamma_{e_hh}=14.5\%$). The radiative recombination rate of optimized three-layer staggered InGa N QW (two-layer staggered InGa N) is calculated as ~ 3.5 times (or 2.4 times) higher than that of conventional InGa N QW. Thus, the use of three-layer staggered InGa N QW over two-layer staggered InGa N QW is important, in particular for extending the emission wavelength into green spectral regime and beyond. Our growth experiments also indicated that the use of three-layer staggered InGa N QW for achieving peak emission wavelength up to 525–550 nm as more practical.

Figure 1(b) shows the calibration studies of the In-content incorporation in MOCVD-grown $\text{In}_x\text{Ga}_{1-x}\text{N}$ layer grown on Ga N template as a function of growth temperature. The growths of InGa N layers employed TMI n , TEGa, and NH_3 as the precursors, and N_2 gas was employed as carrier gas. The V/III and [TMI n]/[TEGa] molar ratios were kept constant at 10200 and 0.38, respectively. The calibrations of the In-contents in the InGa N alloy grown at various growth temperatures were performed by x-ray diffraction measurements. Our studies indicated that the In-content decreases following a relatively linear relation with increasing growth temperature. The In-content in InGa N layer decreases from 28% to 18% as the growth temperature increases from 720 $^{\circ}\text{C}$ to 780 $^{\circ}\text{C}$.

The device characteristics of the three-layer staggered InGa N QW LEDs grown by graded growth-temperature profile were compared to those of the conventional InGa N QW ($\Gamma_{e_hh}=14.5\%$). Both conventional and three-layer staggered InGa N QW were grown by MOCVD on 2.5 μm thick n -doped Ga N ($T_g \sim 1075$ $^{\circ}\text{C}$) grown on c -plane double-side polished sapphire substrate, employing a low temperature 30 nm Ga N buffer layer ($T_g \sim 515$ $^{\circ}\text{C}$). The conventional QW structure consists of four periods 3.5 nm thick $\text{In}_{0.24}\text{Ga}_{0.76}\text{N}$ QWs, which was grown at 740 $^{\circ}\text{C}$ with growth time $t=1.09$ min. The In-content in conventional InGa N QW was calibrated as 24%. The staggered InGa N QW LED consists of four periods of the three-layer staggered InGa N QW. The three-layer staggered InGa N QW consists of three InGa N layers with the higher In-content InGa N layer (layer 2, $T_2=725$ $^{\circ}\text{C}$) in the center sandwiched between two lower In-content InGa N layers (layers 1 and 3, $T_1=755$ $^{\circ}\text{C}$). The growth times for the layers 1, 2, and 3 are $t_1=0.25$ min, $t_2=0.29$ min, and $t_3=0.25$ min, respectively, with the ramp up and ramp down times of $t_p=0.15$ min. From our calibration studies, we estimated the In-contents in the three-layer stag-

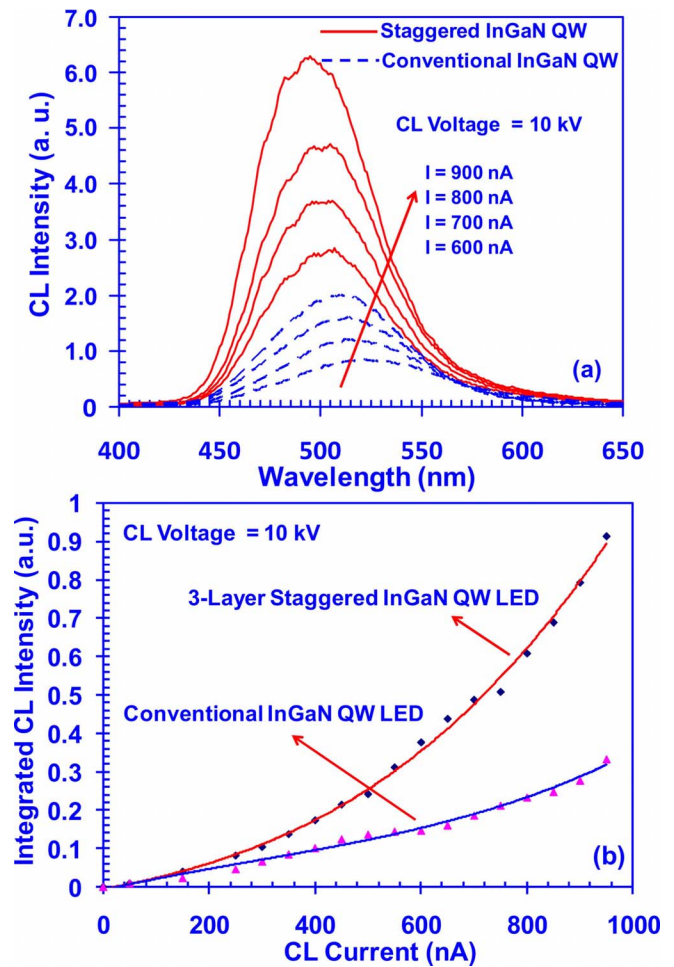


FIG. 2. (Color online) (a) CL spectra and (b) integrated CL intensities of conventional and three-layer staggered InGa N QWs emitting at 520 nm with various CL excitation current at $T=300$ K.

gered InGa N QW as 21%, 28%, and 21%, with thicknesses of 1.05, 1.4, and 1.05 nm, respectively. Both the conventional InGa N QW and three-layer staggered InGa N QW were designed for achieving similar peak emission wavelength in LED operation with nominally similar total QW thickness. All device structures employed 10 nm u -Ga N barrier layer between QW active regions. On top of the upper barrier layer, 200 nm thick p -type Ga N with Mg doping of 3×10^{17} cm^{-3} were grown. The LED devices were fabricated as bottom-emitting square devices, and Ti/Au as n -contact and Ni/Au as p -contact were evaporated followed by contact annealing.

The luminescence characteristics of both the conventional and three-layer staggered InGa N QW samples were studied by power-density-dependent cathodoluminescence (CL) measurements at room temperature. The CL measurements employed 10 keV electron beam in spot mode (area $=1.965 \times 10^{-9}$ cm^2). The high electron beam accelerating energy of 10keV was utilized to penetrate through the 200nm thick p -Ga N layer, which was grown on top of the InGa N QW active region. The effect of different excitation pumping power density on the CL intensity was studied for both of the conventional and three-layer staggered InGa N QW LED samples.

Figure 2(a) shows the measured CL spectra plotted against CL pump current (shown for 600, 700, 800, and 900

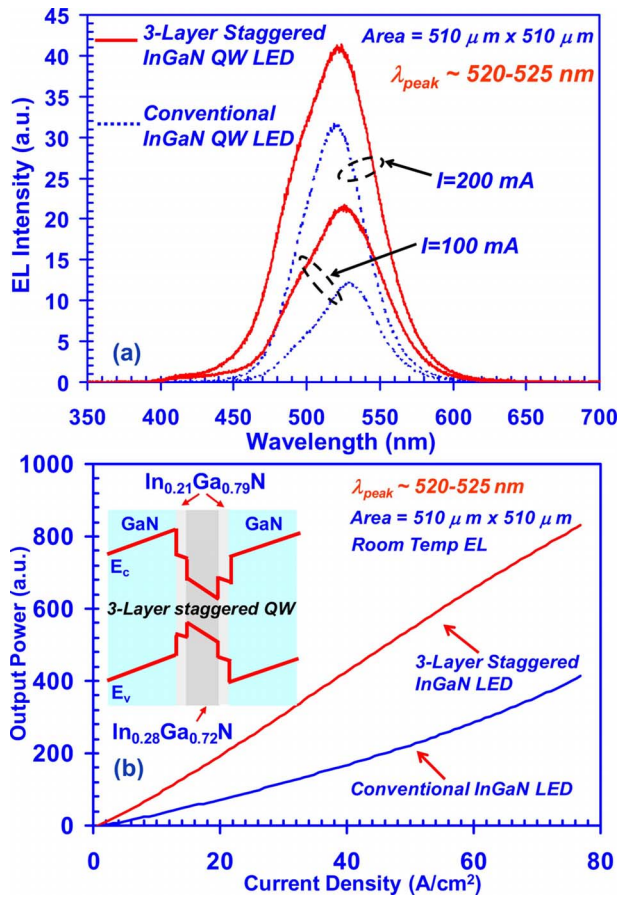


FIG. 3. (Color online) (a) EL spectra and (b) light output power vs current density for conventional InGaN QW and three-layer staggered InGaN QW LEDs emitting with peak wavelengths at 520–525 nm, with the corresponding band lineups schematic of three-layer staggered InGaN QW.

nA) of the conventional and three-layer staggered InGaN QW. The staggered InGaN QW sample exhibits improved peak luminescence by up to approximately 3 times of that of the conventional QW. As shown in Fig. 2(b), the integrated CL intensity of the three-layer staggered InGaN QW exhibit improvement by $\sim 1.8\text{--}2.8$ times compared to that of the conventional QW for CL current from 20 up to 950 nA.

Figure 3(a) shows the electroluminescence (EL) for the conventional InGaN QWs and three-layer staggered InGaN QWs LEDs (area= $510 \times 510\ \mu\text{m}^2$) emitting at 520–525 nm, measured under continuous wave operation. The peak EL for the three-layer staggered InGaN LED shows enhancement by 1.8 times (1.3 times) at $I=100\ \text{mA}$ ($I=200\ \text{mA}$), in comparison to that of conventional InGaN QW LED. The full width at half maximum spectra broadening in three-layer staggered InGaN QW could result from the less abrupt interfaces in QW layer or the increased inhomogeneous broadening in higher In-content InGaN layer.

Figure 3(b) shows the output power versus the injected current density for conventional and three-layer staggered

InGaN LEDs. The enhancement in both radiative efficiency and output power of the three-layer staggered InGaN QW LEDs indicated that the increase in radiative recombination rate from the improved electron-hole wave function as a dominant contributing factor to the improved device characteristics. The output power of the three-layer staggered InGaN QW LED was measured as 2.0–3.5 times higher in comparison to that of conventional InGaN QW LED [Fig. 3(b)]. The improvement observed from our experimental results for green-emitting staggered InGaN QW LEDs is in good agreement with the recent theoretical results.^{14,18}

In summary, the use of three-layer staggered InGaN QWs resulted in improved active region for nitride LEDs emitting at 520–525 nm. The power dependent CL measurement indicated 1.8–2.8 times enhancement for the three-layer staggered InGaN QW. The output power and radiative efficiency of three-layer staggered InGaN QW LED improved by 2.0–3.5 times, in comparison to those of conventional InGaN QW LED. The improvement in radiative efficiency of three-layer staggered InGaN QW LED can be attributed to the increase in radiative recombination rate of the QW, in agreement with theory.

The authors would like to acknowledge funding supports from U.S. Department of Energy (Grant No. DE-FC26-08NT01581) and U.S. National Science Foundation (Grant No. ECCS # 0701421).

- ¹S. Nakamura, M. Senoh, S. Nagahama, N. Iwasa, T. Yamada, T. Matsushita, H. Kiyoku, and Y. Sugimoto, *Jpn. J. Appl. Phys., Part 2* **35**, L74 (1996).
- ²J. Zhang, J. Yang, G. Simin, M. Shatalov, M. A. Khan, M. S. Shur, and R. Gaska, *Appl. Phys. Lett.* **77**, 2668 (2000).
- ³X. Guo, Y. L. Li, and E. F. Schubert, *Appl. Phys. Lett.* **79**, 1936 (2001).
- ⁴Y. K. Ee, P. Kumnorakaw, R. A. Arif, J. F. Gilchrist, and N. Tansu, *Appl. Phys. Lett.* **91**, 221107 (2007).
- ⁵R. M. Farrell, D. F. Feezell, M. C. Schmidt, D. A. Haeger, K. M. Kelchner, K. Iso, H. Yamada, M. Saito, K. Fujito, D. A. Cohen, J. S. Speck, S. P. DenBaars, and S. Nakamura, *Jpn. J. Appl. Phys., Part 2* **46**, L761 (2007).
- ⁶J. Park and Y. Kawakami, *Appl. Phys. Lett.* **88**, 202107 (2006).
- ⁷S. H. Park, J. Park, and E. Yoon, *Appl. Phys. Lett.* **90**, 023508 (2007).
- ⁸R. A. Arif, Y. K. Ee, and N. Tansu, *Appl. Phys. Lett.* **91**, 091110 (2007).
- ⁹R. A. Arif, H. Zhao, Y. K. Ee, and N. Tansu, *IEEE J. Quantum Electron.* **44**, 573 (2008).
- ¹⁰R. A. Arif, H. Zhao, and N. Tansu, *Appl. Phys. Lett.* **92**, 011104 (2008).
- ¹¹H. Zhao, R. A. Arif, and N. Tansu, *J. Appl. Phys.* **104**, 043104 (2008).
- ¹²H. Zhao, R. A. Arif, Y. K. Ee, and N. Tansu, *Opt. Quantum Electron.* **40**, 301 (2008).
- ¹³H. Zhao, R. A. Arif, Y. K. Ee, and N. Tansu, *IEEE J. Quantum Electron.* **45**, 66 (2009).
- ¹⁴H. Zhao, R. A. Arif, and N. Tansu, *IEEE J. Sel. Top. Quantum Electron.* **15**, 1104 (2009).
- ¹⁵S. L. Chuang and C. S. Chang, *Semicond. Sci. Technol.* **12**, 252 (1997).
- ¹⁶S. L. Chuang and C. S. Chang, *Phys. Rev. B* **54**, 2491 (1996).
- ¹⁷S. L. Chuang, *Physics of Optoelectronics Devices* (Wiley, New York, 1995), Chaps. 4 and 9.
- ¹⁸S. H. Park, D. Ahn, and J. W. Kim, *Appl. Phys. Lett.* **94**, 041109 (2009).